Liao, X., Fang, J., Zhao, X., Song, W., Yang, S. and Sun, Y. (2022) Analysis of electromagnetic characteristics of 6.5 MVA/25 kV HTS traction transformer using T-A formulation. IEEE Transactions on Applied Superconductivity, (doi: 10.1109/TASC.2022.3190365).

There may be differences between this version and the published version. You are advised to consult the publisher's version if you wish to cite from it.

https://eprints.gla.ac.uk/275391/

Deposited on: 22 July 2022

Enlighten – Research publications by members of the University of Glasgow
http://eprints.gla.ac.uk

Analysis of Electromagnetic Characteristics of 6.5 MVA/25 kV HTS Traction Transformer Using T-A Formulation

Xu Liao, Jin Fang, Xin Zhao, Member, IEEE, Wenjuan Song, Song Yang, Yueming Sun

***Abstract*—Low AC loss of the winding of high-capacity high temperature superconducting (HTS) traction transformer is a very important link to introduce large capacity traction transformer into commercialization. A new winding structure is proposed for the transformer. The HV windings are made of double pancake coils (DPCs), which are wound by 4.8 mm-wide tapes, and the LV windings, which are wound by 12 mm-wide tapes, are solenoid coils. The electromagnetic characteristics of the new winding structure of the traction transformer are analyzed by *H*-formulation homogenization method and *T-A* formulation homogenization method respectively. Significant HTS tape cost reduction could be achieved without compromising AC loss by using hybrid windings into the new winding structure. We report that the *H*-formulation homogenization model and *T-A* formulation homogenization model are used to calculate the AC loss of the new winding structure with flux diverters (FDs) at the end. The results meet the design requirements of less than 2 kW, which shows the feasibility of the new winding structure. Due to the good convergence of *H*-formulation and poor convergence of *T-A* formulation under the homogenization model of the transformer, no one has used *T-A* formulation to calculate the electromagnetic characteristics of the transformer before. Due to the simplicity of *T-A* formulation applied to large-scale superconducting system, a new form of mesh generation is proposed to improve the convergence and accuracy of *T-A* formulation homogenization model calculation of the transformer in this paper. This paper verifies the correctness of the calculation of HTS transformer by *T-A* formulation, and provides a reference for the application of *T-A* formulation in more superconducting fields.**

***Index Terms*—HTS traction transformer, electromagnetic characteristic analysis, *T-A* formulation, hybrid winding structure**

I. Introduction

Compared with traditional transformers, HTS transformers have the advantages of low loss, high efficiency, reduced volume and weight, reduced potential fire and environmental hazards. When the HTS transformer operates at power frequency, it will produce AC loss, which will lead to temperature rise. In serious cases, it will lead to quench of superconductors and damage the equipment. Therefore, it is very important for the design and industrialization of superconducting transformer to accurately calculate the AC loss of HTS transformer. Over the past decade, research groups have been designing, manufacturing and testing HTS transformers used in various fields [1-4]. Since 2018, Beijing jiaotong University has been leading a six-party cooperation project to develop a 6.5 MVA HTS traction transformer for high-speed trains. Up to now, the transformer prototype is in the processing stage. Among them, the refrigeration system of the transformer will be cooled by refrigeration mechanism. The HTS transformer is expected to perform better than traditional transformers with oil-immersed copper windings, achieving 99% efficiency and 3 tons of total system weight, whereas traditional transformers are 95% efficient and weigh approximately 6 tons.

The transformer is composed of four single-phase 25 kV/1.9 kV HTS windings, operating at 50 Hz under the temperature of 65 K provided by the refrigerator, each of which drive a motor. The overall structure of the transformer is shown in Fig. 1. The winding structure proposed at the beginning of the transformer is described in [5]. The HV windings are wound with 4 mm-wide tapes, and the LV windings are wound with 8/5 (eight 5 mm-wide strands) Roebel cable. As the technology of Roebel cable is not yet fully mature, the project team cannot produce Roebel cable in such a large scale to be applied to the transformer. Therefore, the project team proposes a new winding form. The HV windings are wound into double pancake coils with 4.8 mm-wide tapes, and the LV windings are wound into solenoids after two 12 mm-wide tapes with insulation are connected in parallel. As shown in Fig. 2, the traction transformer has four winding units, each unit is composed of a HV winding and two LV traction windings, of which the two LV windings are in parallel connection with the same number of ampere turns. According to the winding structure in [5], the rated currents for each of HV and LV winding are 64.5 A and 846 A respectively. According to the new winding structure, the rated current of HV winding of each unit is still 64.5 A, while both two parallel LV traction windings of each unit are 423 A. Therefore, this winding structure can also make the LV winding achieve the effect of current sharing when the current capacity meets the requirements. All windings

This work was supported by Ministry of Science and Technology on National Key Research and Development Program under Grant 2016YFE0201200. (Corresponding author: Jin Fang.)

Xu Liao, Jin Fang, Xin Zhao, Song Yang, Yueming Sun, Yue Wu are with the School of Electrical Engineering, Beijing Jiaotong University, Beijing 100044, China (e-mail: jfang@bjtu.edu.cn).

Wenjuan Song is with the James Watt School of Engineering, The University of Glasgow, Glasgow, GB.

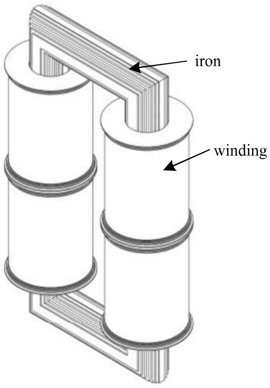

Fig. 1. Overall structure of 6.5 MVA 25 kV/1.9 kV HTS traction transformer

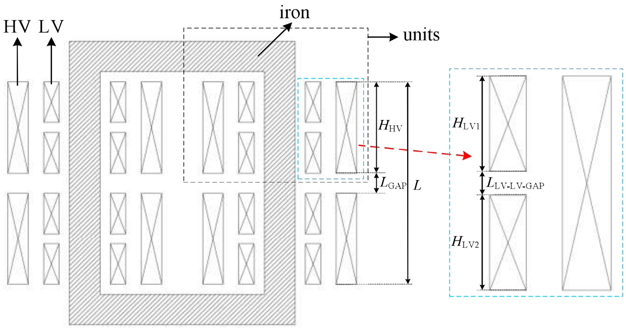

Fig. 2. New winding structure of 6.5 MVA 25 kV/1.9 kV HTS traction transformer

TABLE I
Specifications of winding design

Winding	LV winding		HV winding
	Winding 1	Winding 2	
Number of total turns	149	149	1961
Number of discs	19	19	45
Inner diameter (mm)	290	290	420
Outer diameter (mm)	310	310	446
Radial thickness (mm)	10	10	13.5
Axial height (mm)	287.5	287.5	585

are separately encapsulated in vacuum Dewar and cooled by sub-cooled liquid nitrogen. Table I lists the design specifications of the HV and LV windings.

The FEM models of HTS tapes use different Maxwell's equations, and the difference between the formulations depends on the different state variables. Maxwell equations have many forms used to simulate the FEM models of HTS systems, but the most commonly used are *H*-formulation and *T-A* formulation. The first is the most common *H*-formulation, which is applied in many research fields, such as superconducting motor [6], superconducting transformer [5], [7-8], superconducting cable [9], superconducting flux pump [10], superconducting fault current limiter [11], superconducting magnetic energy storage [12]; The second is to propose in [13-14] that *T-A* formulation is an effective method to simulate thin layer of superconductor. This method couples *T* and *A* formulations and can effectively solve the analysis of large-scale HTS systems. With the further study of *T-A* formulation [15], the application field of *T-A* formulation has become more and more widely, including superconducting motor [16-17], superconducting fault current limiter [18], superconducting cable [19], superconducting flux pump [20]. However, the application of *T-A* formulation in superconducting transformer has not been involved. In this paper, the electromagnetic analysis of 6.5 MVA HTS traction transformer is carried out by *T-A* formulation for the first time, and compared with *H*-formulation. *H*-formulation has been widely used since it was proposed. However, due to *H*-formulation is more cumbersome in modeling, its effect in large-scale HTS system is not very ideal. On the contrary, the modeling process *T-A* formulation is much simpler than *H*-formulation, which is very convenient for the modification of the models of large-scale HTS systems. Therefore, the application of *T-A* formulation to HTS transformer can also have a very good result.

In this paper, we use *H*-formulation and *T-A* formulation to establish the homogenization model of the HTS traction transformer under the new winding structure, and complete the calculation and the comparative analysis of electromagnetic characteristics between the two models. The tape of transformer winding has high critical current and high-quality Fujikura tapes with a self-field critical current of 1140 A/cm at 65 K, and Shanghai Superconductor (SHS) tapes with critical current and lower price, the self-field critical current of 12 mm-wide tapes at 65 K is 975 A, and the self-field critical current of 4.8 mm-wide tapes at 65 K is 355 A. Fig. 9 shows the AC loss distribution of HV and LV windings calculated only by Fujikura tape or SHS tape. Through the comparison results, a winding hybrid tape structure is proposed. Finally, with flux diverters arranged at the outer ends of the windings of this hybrid configuration, we calculate the AC loss, which is less than our AC loss target for the project.

II. Numerical Calculation

Calculations have been carried out in two-dimensional axisymmetric coordinate system using *T-A* formulation homogenization method. Considering the four winding units of the transformer are symmetrically distributed, only one winding unit needs to be analyzed. Fig. 3 shows the schematic of a quarter 2D axisymmetric model for the transformer windings.

As shown in Fig. 4, *A* formulation needs to be used in both the superconducting domain and the air domain, while *T* formulation is only used in the superconducting domain. The current vector potential **T** is only defined in the superconducting domain, while the magnetic vector potential **A** is defined over the entire bounded universe.

Firstly, the current vector potential **T** and magnetic vector potential **A** are defined as,

$$\mathbf{J} = \nabla \times \mathbf{T} \tag{1}$$

$$\mathbf{B} = \nabla \times \mathbf{A} \tag{2}$$

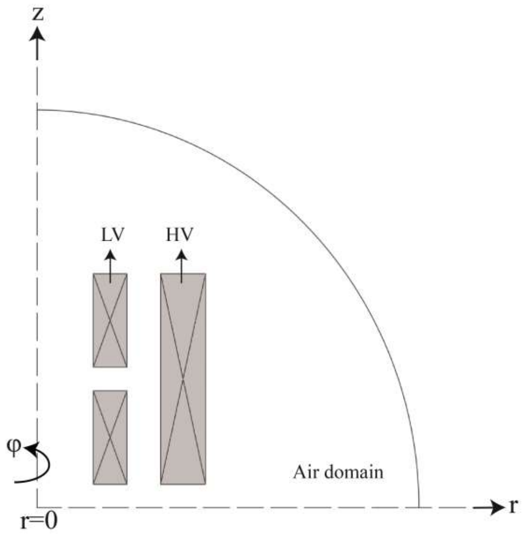

Fig. 3. Schematic of a 2D axisymmetric model for 6.5 MVA transformer (only a quarter model was simulated).

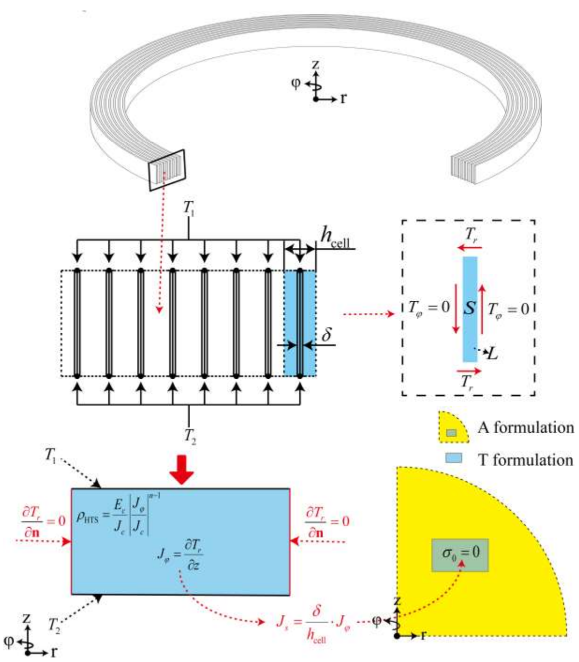

Fig. 4. Calculation principle of *T-A* formulation homogenization method

The governing equation of the A formulation is

$$\nabla^2 \mathbf{A} = -\mu_r \mu_0 \mathbf{J} \tag{3}$$

where μ_r is the relative permeability, μ_0 is vacuum permeability.

The governing equation of the *T* formulation is

$$\nabla \times \rho \nabla \times \mathbf{T} = -\frac{\partial \mathbf{B}}{\partial t} \tag{4}$$

where ρ is the resistivity, and **B** is defined as $\mathbf{B} = \nabla \times \mathbf{A}$, where **B** is the magnetic flux density.

The superconducting tapes are approximated as a one-dimensional thin layer in the *T-A* formulation calculation model, and the transport current can only flow on the line. Therefore, the vector **T** can only have one component T_r. The superconducting tapes are still treated as one-dimensional thin layers, so the vector **T** can only have one component T_r. Although the superconducting thin layer is replaced by the superconducting domain, the current can only flow along the line parallel to the original superconducting thin layer. The homogenized superconducting bulk can be regarded as the compressed composition of countless superconducting thin layers, so the whole transport current can only be treated as countless line currents. Therefore, equation (4) is simplified to obtain

$$\frac{\partial}{\partial z}\left(\rho_{HTS}\frac{\partial T_r}{\partial z}\right) = \frac{\partial B_r}{\partial t} \tag{5}$$

where ρ_{HTS} is the resistivity of superconductor, which is modeled by *E-J* power law as shown as (6) to indicate the resistivity for superconducting tape.

$$\rho_{\mathrm{HTS}} = \frac{E_c}{J_c(B)}\left|\frac{J_\varphi}{J_c(B)}\right|^{n-1} \tag{6}$$

Here, the power index n = 25, E_c = 10^{-4} V/m. $J_c(B)$ is the critical current density dependent on the applied magnetic field, which can be obtained by dividing the measured value of $I_c(B)$ by the cross-sectional area *S* of the superconductor.

By simplifying the definition equation (1) of the current vector potential **T**, it is obtained that the current density **J** is only J_φ one component

$$J_\phi = \frac{\partial T_r}{\partial z} \tag{7}$$

A_φ can be obtained by substituting J_φ into the governing equation of *A* formulation. B_r can be obtained through the definition equation (2) of the vector **A**. Finally, the solution can be completed by substituting both of them into the governing equation of *T* formulation.

The necessary boundary conditions at the edges of the 1D superconducting layer for **T** can be obtained by integrating the current density **J** over the cross-section of the layer which is equal to the transport current in the tape, as follows,

$$I = \iint_S \mathbf{J} \mathrm{d}S = \iint_S \nabla \times \mathbf{T} \mathrm{d}S = \oint_L \mathbf{T} \mathrm{d}\Phi \tag{8}$$

where *S* is the cross-section of the superconductor and *L* is its boundary. As shown in Fig. 4, the component **T** parallel to the superconducting layer is T_φ=0, then equation (8) is simplified as

$$I = (T_1 - T_2)\delta \tag{9}$$

where δ is the real thickness of the superconducting layer. T_1 and T_2 are the potentials at the extremities of the 1D layer as shown in Fig. 4. Thus, a different transport current can be applied to superconducting tapes by modifying T_1 and T_2.

After homogenization modeling, the whole homogenized conductor domain is regarded as a whole, and the external transmission current is also applied by applying surface current density to the whole superconducting domain. At this time, the superconducting tapes are regarded as a rectangular superconducting domain with width of w_{tape} and thickness of h_{cell} under the A formulation, but the superconducting domain should be equivalent to the real thickness of δ. Therefore, the current density under A formulation and the current density under T formulation should meet the relationship of equation (10).

$$J_\varphi \cdot \delta = J_{\text{e}} \cdot h_{\text{cell}} \tag{10}$$

where h_{cell} is the thickness of unit cell, J_{e} is the external current density, J_φ is the current density under T formulation. The J_{e}, for the purpose of computing A_φ, is impressed in the bulk domain as a source term as follows

$$\nabla^2 A_\varphi = -\mu_0 \left(\sigma_0 E_\varphi + J_{\text{e}}\right) \tag{11}$$

where σ_0 is the conductivity of the surrounding medium, which is considered as the conductivity of the entire bounded universe.

Finally, we have to establish the boundary conditions to solve our problem. The homogenized bulk represents a densely packed group of HTS sheets. Each one of these sheets should transport the same current as its original counterpart [21]. Therefore, we apply Dirichlet boundary conditions to the upper and lower gray boundaries as expressed in equation (8) and apply Neumann boundary conditions to the internal and external boundaries:

$$\frac{\partial T_r}{\partial \mathbf{n}} = 0 \tag{12}$$

Where $\mathbf{n}$ is the unit vector perpendicular to the boundary.

III. Result and Discussion

For the case that Fujikura tapes are used for the whole HV and LV windings, the LV windings adopt 12 mm-wide tapes with a self-field critical current is 1140 * 1.2 = 1368 A at 65 K; the HV windings adopt 4.8 mm-wide tapes with a self-field critical current is 1140 * 0.48 = 547.2 A at 65 K. For the case that Fujikura tapes are used for the whole HV and LV windings, the LV windings adopt 12 mm-wide tapes with a self-field critical current is 975 A at 65 K; the HV windings adopt 4.8 mm-wide tapes with a self-field critical current is 355 A at 65 K. Both tapes show strong anisotropy, so in order to get more accurate simulation results, the magnetic field dependence of critical current is fully considered in the simulation model. We used the modified Kim model [22] in the simulation for J_{c}(B) performance, as shown in equation (13),

$$J_{\text{c}}\left(\mathbf{B}\right) = \frac{J_{\text{c0}}}{\left(1 + \dfrac{k^2 B_{/\!/}^2 + B_\perp^2}{B_0^2}\right)^\alpha} \tag{13}$$

Here, $B_\perp$ is the radial magnetic field B_{r}, $B_{/\!/}$ is the axial magnetic field B_z.

As for Fujikura tape, three parameters, k = 0.71, B_0 = 100 mT and α = 0.23 are characteristics associated with magnetic field dependence of the materials [3].

However, for SHS tape, the magnetic field dependence of the critical current at 65 K for two tapes with 4.8 mm-wide tapes for the HV windings and 12 mm-wide tapes for the LV windings is shown in Fig. 5. By fitting the measured data in Fig. 5, the three characteristic parameters of 4.8 mm-wide SHS tapes are k = 0.613, B_0 = 73 mT and α = 0.34, and the three characteristic parameters of 12 mm-wide SHS tapes are k = 0.62, B_0 = 60 mT and α = 0.24.

A DPCs model composed of two different SHS tapes is

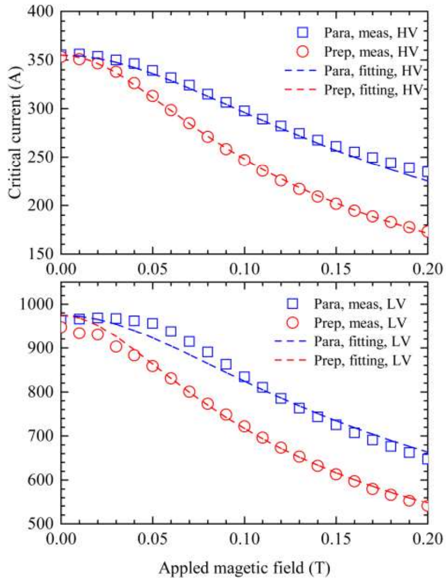

Fig. 5. Dependence of critical current on magnetic field for two kinds of SHS tapes at 65K

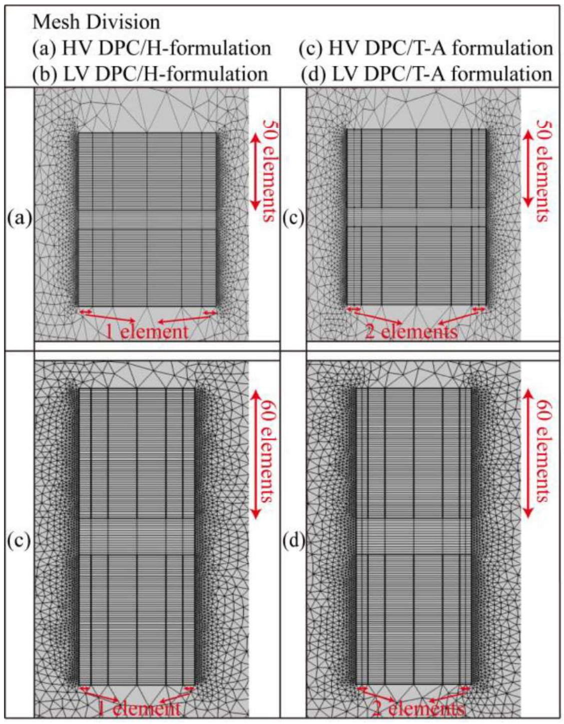

Fig. 6. Mesh generation of a DPC composed of two kinds of tapes in SHS tape

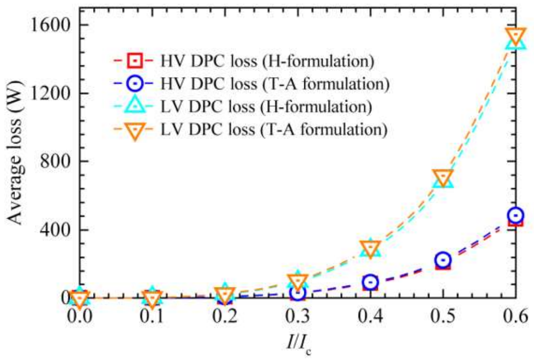

Fig. 7. Calculation results of average AC loss of SHS tape DPC composed of two kinds of tapes when the current amplitude is 0.1 - 0.6 I_c

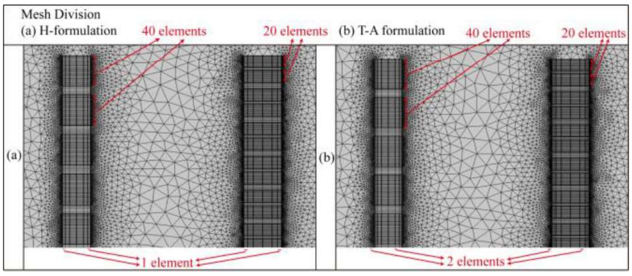

Fig. 8. Mesh generation of new winding structure of 6.5 MVA traction transformer (a)H-formulation (b)T-A formulation

established by using *H*-formulation homogenization model and *T-A* formulation homogenization model respectively. The convergence of *H*-formulation homogenization model is very well, so there is no high requirement for mesh generation. It can have good convergence by using the form of mesh generation in Fig. 6(a) and 6(b). However, for the *T-A* formulation homogenization model, the form of mesh generation in Fig. 6(a) and 6(b) has poor convergence or even non convergence. In order to solve the problem of poor convergence of *T-A* formulation homogenization model, this paper proposes a new form of mesh generation in Fig. 6(c) and 6(d). Through calculation, it is found that the form of mesh generation can improve the convergence of the model, has no impact on the calculated magnetic field distribution and current density distribution, and can also improve the accuracy of AC loss calculation. For the large-scale superconducting system such as HTS transformer, the homogenization model is generally recommended for modeling, and the technology of modeling it with *H*-formulation homogenization model has been very mature, but the application of *T-A* formulation homogenization model in HTS transformer is hardly involved. Therefore, we believe that when the *T-A* formulation homogenization model is used to calculate the HTS transformer, good calculation results can be obtained by using the form of mesh generation in Fig. 6(c) and 6(d). Fig. 7 shows the average AC loss calculation value of DPCs composed of two different SHS tapes when the current amplitude is 0.1 - 0.6 I_c. It can be seen from the figure that the calculation results of *H*-formulation homogenization model and *T-A* formulation homogenization model are very close, which indirectly illustrates the correctness of the establishment of *T-A* formulation homogenization model.

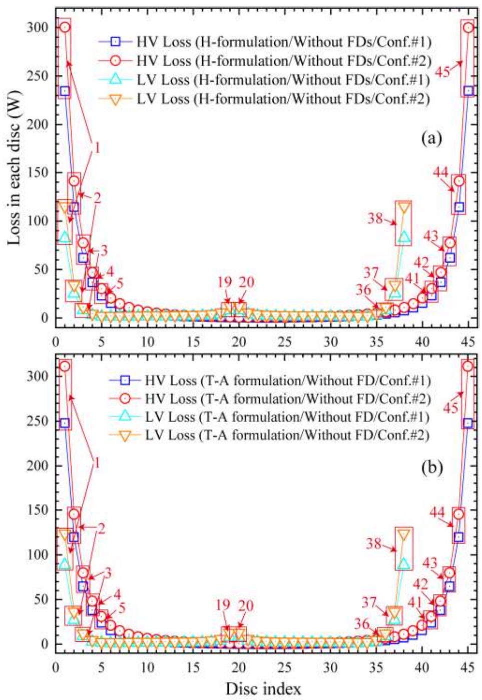

Fig. 9. Comparison of AC loss in each disc when only Fujikura tape or SHS tape is used for HV and LV windings

Fig. 8 shows the mesh generation of the new winding structure of 6.5 MVA traction transformer. The form of mesh generation of *H*-formulation homogenization model is the same as that in Fig. 6(a) and 6(b). The form of mesh generation of *T-A* formulation homogenization model adopts the newly proposed method, and the division results are shown in Fig. 8(b).

For the multi-coils winding wound from the same superconducting tapes, the end coils of the winding usually produce higher AC loss compared with the central coils due to the larger local perpendicular magnetic field component. To reduce AC loss of windings, superconducting tapes with higher critical current capacity are used for the end coils based on the fact that the higher the critical current of the superconducting tape is, the lower AC loss. Such a hybrid tape method can effectively reduce the winding AC loss with a reasonable material cost. In addition, previous study demonstrated and reported the measured AC loss results on the hybrid winding approach in [8, 23], and the mechanism has been verified experimentally and numerically. Fig. 9(a) shows that the comparative analysis of the average AC loss in each disc of when the HV and LV windings calculated by *H*-formulation are used Fujikura tapes or SHS tapes. It can be seen that for HV discs with index numbers of 1,2,3,4,5,41,42,43,44,45, the AC loss values of two different tapes vary greatly. Similarly, for LV discs with index numbers of 1,2,3,19,20,36,37,38, the AC loss values of two different tapes also vary greatly. For HV/LV discs with other index numbers, the average AC loss values of the two different tapes are very close. Therefore, in order to reduce

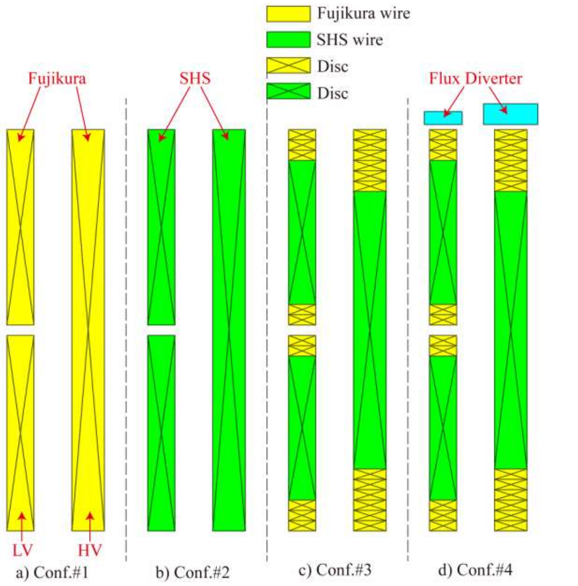

Fig. 10. Schematics of hybrid transformer windings a) Conf. #1 b) Conf. #2 c) Conf. #3 d) Conf. #4

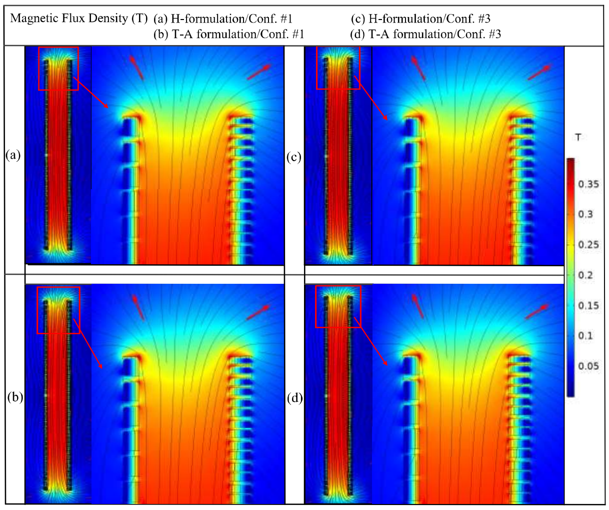

Fig. 11. Magnetic flux density distribution of transformer quarter calculation model (a) *H*-formulation/Conf. #1 (b) *T-A* formulation/Conf. #1 (c) *H*-formulation/Conf. #3 (d) *T-A* formulation/Conf. #3

HTS tape cost and meet the requirements of AC loss, a hybrid coil winding structure can be introduced in the traction transformer. Obviously, Fujikura tape with high I_c and higher cost is used for HV discs with index numbers of 1,2,3,4,5,41,42,43,44,45 and LV discs with index numbers of 1,2,3,19,20,36,37,38, while SHS tape with low I_c and lower cost is used for HV/LV discs with other index numbers. The simulation results using *T-A* formulation are shown in Fig. 9(b). Obviously, the law obtained by the simulation using *T-A* formulation is the same as that using *H*-formulation. For the case that only Fujikura tapes are used for both HV and LV windings, the total AC loss of a pair of windings calculated by *H*-formulation is 1367.83 W, and the total AC loss of a pair of windings calculated by *T-A* formulation is 1427.77 W, with a calculation error of 4.38%. For the case that only SHS tapes are used for both HV and LV windings, the total AC loss of a pair of windings calculated by *H*-formulation is 1804.52 W, and the total AC loss of a pair of windings calculated by *T-A* formulation is 1873.54 W, with a calculation error of 3.68%.

We designed four configurations for transformer windings including two hybrid windings. The schematics of the windings are shown in Fig. 10. In Conf. #1, HV and LV windings are wound with Fujikura tape only. In Conf. #2, HV and LV windings are wound with SHS tape only. In Conf. #3, HV discs with index numbers of 1,2,3,4,5,41,42,43,44,45 and LV discs with index numbers of 1,2,3,19,20,36,37,38 adopt Fujikura tape, while HV/LV discs with other numbers adopt SHS tape. Conf. #4 is the same as Conf. #3 except for the flux diverters arranged near the end of the windings.

Since the total AC loss on a pair of windings of winding form of Conf. #2 cannot meet the project requirements of AC loss less than 500W, only Conf. #1 and Conf. #3 are compared here. Fig. 11 shows the magnetic field distribution of transformer winding in Conf. #1 and #3 cases calculated by *H*-formulation and *T-A* formulation respectively. As can be seen from Fig. 11(a) and Fig.

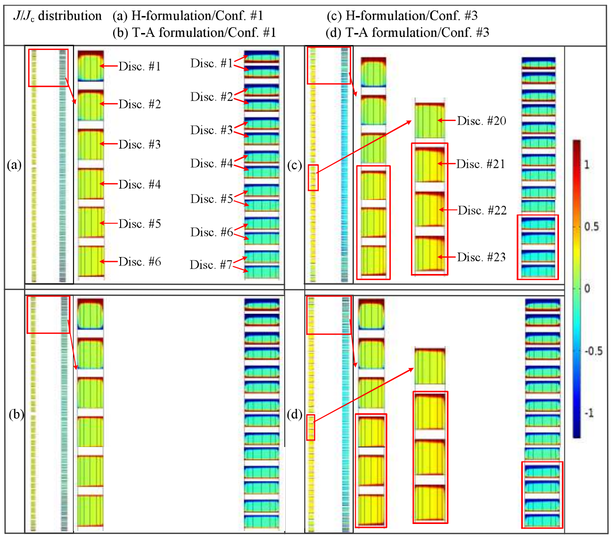

Fig. 12. J/J_c distribution of transformer quarter calculation model (a) *H*-formulation/Conf.#1 (b) *T-A* formulation/Conf.#1 (c) *H*-formulation/Conf.#3 (d) *T-A* formulation/Conf.#3

11(c), the use of hybrid winding does not influence the magnetic field distribution and magnitude. The magnetic field at the end of windings reaches the maximum, and the maximum value is 0.395 T. According to the $J_c(B)$ formulation of equation (8), the coils at the end of the windings are greatly affected by the magnetic field, so the critical current of the coils at the end the windings is the lowest. Fig. 11(b) and Fig. 11(d) show the magnetic field distribution calculated by *T-A* formulation corresponding to Fig. 11(a) and Fig. 11(c) respectively. It can be seen that the magnetic field distribution calculated by *T-A* formulation is basically, consistent with that calculated by *H*-formulation.

Fig. 12 shows the J/J_c distribution of the transformer winding in

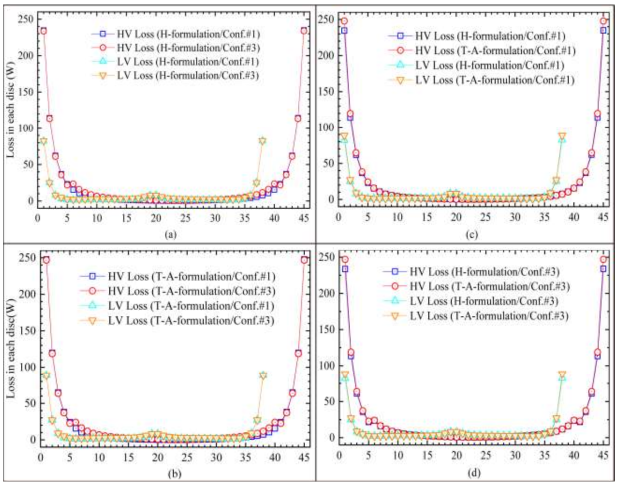

Fig. 13 the distribution and comparative analysis of AC loss in each disc of HV and LV winding of transformer winding in Conf. #1 and Conf. #3 cases calculated by *H*-formulation and *T-A* formulation respectively (a) *H*-formulation (Conf.#1 vs Conf.#3) (b) *T-A* formulation (Conf.#1 vs Conf.#3) (c) Conf.#1 (*H*-formulation vs *T-A* formulation) (d) Conf.#1 (*H*-formulation vs *T-A* formulation)

Conf. #1 and Conf. #3 cases calculated by *H*-formulation and *T-A* formulation respectively. It can be seen from the figure that the J/J_c distribution is symmetrical from the end of the winding to the center. For the case that only Fujikura tapes are used for HV and LV windings, it can be seen from Fig. 12(a) that HV/LV discs extends from both ends to the center, and the region of $|J/J_c| > 1$ is gradually decreasing. Due to the large radial component of the magnetic field at the end of the windings and the large attenuation of the critical current of the coils at the end of the windings, the region of $|J/J_c| > 1$ is very big. And there is shielding current flowing opposite to coil current at the bottom of several discs at the end of HV and LV windings in order to shield the radial magnetic field component in the end part of the windings. For the case that mixed tapes are used for HV and LV windings, it can be seen from Fig. 12(b) that when the disc index number of the HV winding ranges from 1 to 5, the region of $|J/J_c| > 1$ gradually decreases, but when it reaches Disc.# 6, the region of $|J/J_c| > 1$ suddenly increases and extends from Disc.# 6 to the center, then the region of $|J/J_c| > 1$ gradually decreases again. For the LV winding, the same law as the HV winding is satisfied. The critical current of SHS tape is much lower than that of Fujikura tape, so the J/J_c distribution accords with the actual situation when mixed tapes are used in the windings. Fig. 12(b) and 12(d) show the J/Jc distribution calculated by *T-A* formulation corresponding to Fig. 12(a) and 12(c) respectively. It can be seen that the J/J_c distribution calculated by *T-A* formulation is basically consistent with that calculated by *H*-formulation.

Fig. 13 shows the distribution and comparative analysis of AC loss in each disc of HV and LV winding of transformer winding in Conf. #1 and Conf. #3 cases calculated by *H*-formulation and *T-A* formulation respectively. Fig. 13(a) shows the distribution of AC loss in each disc of high and HV and LV winding of transformer

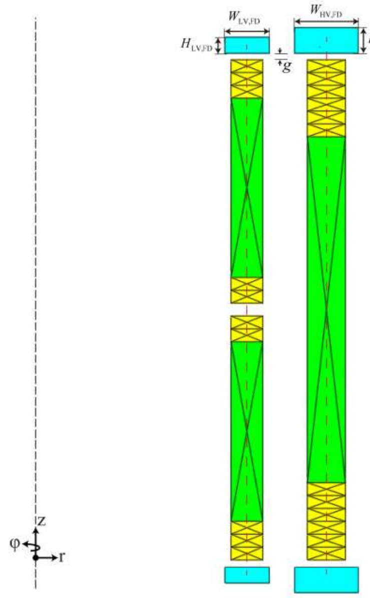

Fig. 14. Schematic of FDs in HV and LV winding of 1/4 transformer model

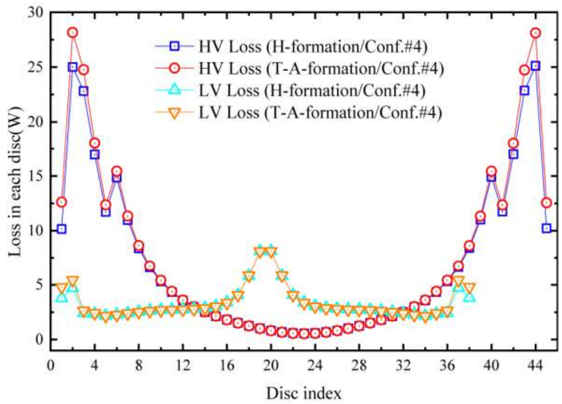

Fig. 15. Calculation of AC loss distribution in HV and LV winding with FDs to the 1/4 transformer model

winding in Conf. #1 and Conf. #3 cases calculated by *H*-formulation. It can be seen that after the windings use mixed tapes, the AC loss in the disc originally using Fujikura tape remains unchanged, while the AC loss in the disc using SHS tape increases slightly. However, compared with the windings only using Fujikura tapes, the increase of AC loss will not have a great impact, but the HTS tape cost can be greatly reduced. Fig. 13(b) shows the results of *T-A* formulation calculation corresponding to Fig. 13(a). It can be seen that the results and laws calculated by the two methods are basically the same. Fig. 13(c) and 13(d) shows the distribution of AC loss in each disc of HV and LV winding of transformer winding in Conf. #1 case calculated by *H*-formulation and *T-A* formulation respectively. For Conf. #1, the total AC loss of a pair of windings calculated by H-formulation is 1367.83 W, and the total AC loss of a pair of windings calculated by *T-A* formulation is 1427.77 W, with a calculation error of 4.38%. For

Conf. #3, the total AC loss of a pair of windings calculated by *H*-formulation is 1464.44 W, the total AC loss of a pair of windings calculated by *T-A* formulation is 1526.98 W, and the calculation error is 4.27%. Through the calculation results, it can be seen that the total AC loss of the winding with hybrid tape increases a little compared with that with Fujikura tape only, but the loss reduction is very considerable compared with that with SHS tape only. This also shows that the use of mixed tapes for winding can greatly reduce the tape cost under the condition of meeting the design requirements of AC loss.

Fig. 14 shows the schematic of dimensions for flux diverters arranged near the outer ends of the HV and LV windings of Conf. #3. Here, the cross-section of flux diverter was chosen as rectangle and the permeability of magnetic material in the flux diverter has a constant μ_r of 100. The shape parameters $W_{HV,FD}$, $H_{HV,FD}$, $W_{LV,FD}$, and $H_{LV,FD}$ of FDs are 30 mm, 12 mm, 23 mm and 8 mm respectively, and its position parameter g is 2.5 mm.

Fig. 15 shows the distribution and comparative analysis of AC loss in each disc of HV and LV winding of transformer winding in Conf. #4 case calculated by *H*-formulation and *T-A*-formulation respectively. It can be seen that after adding FDs, the AC losses of end coils of HV and LV windings are significantly reduced compared with that without adding FDs. Under the rated current, the total AC loss of a pair of windings calculated by *H*-formulation is 440.47 W, and the total AC loss of four pairs of windings of the corresponding transformer is 1761.88 W, less than 2 kW; The total AC loss of a pair of windings calculated by *T-A* formulation is 464.40 W, and the total AC loss of four pairs of windings of the corresponding transformer is 1857.60 W, which is also less than 2 kW. The calculation error of the two methods is 5.43%.

Through the above comparative analysis of the electromagnetic characteristics of HTS traction transformer calculated by *H*-formulation and *T-A* formulation, it can be found that the calculation results using *T-A* formulation are basically consistent with those using *H*-formulation, which also shows the correctness of the calculation of the finite element model. Compared with *H*-formulation model, *T-A* formulation model is much simpler in modeling. For the HTS traction transformer model described in this paper, it often takes 5-6 hours for *H*-formulation model to complete modeling, while it may only take 2-3 hours to use *T-A* formulation model, and the simulation calculation time difference between the two methods is not very long. The only difference is that the memory of *T-A* formulation model after simulation calculation is twice that of *H*-formulation model. Considering comprehensively, *T-A* formulation calculation method has greater advantages than *H*-formulation calculation method.

IV. CONCLUSIONS

In this paper, the electromagnetic characteristics of 6.5 MVA 25 kV/1.9 kV traction transformer are analyzed by *T-A* formulation homogenization model for the first time, and compared with the calculation results of *H*-formulation homogenization model. The calculation results show the correctness of *T-A* formulation homogenization model.

By comparing the AC loss in each disc when only Fujikura tape is used for the HV and LV windings of the transformer with that when only SHS tape is used, we choose a hybrid tape method of using Fujikura tape and SHS tape at the same time, which can greatly reduce the winding tape cost and the AC loss can meet the required requirements. Finally, by adding FDs at the ends of HV and LV windings, the total AC loss of four pairs of windings of the transformer is reduced to about 1.8 kW, meeting the requirements of less than 2 kW.

For the large-scale superconducting system such as large-capacity superconducting transformer, using *H*-formulation model for calculation will take a long time in the process of establishing the model, while using *T-A* formulation model for calculation can well solve this problem and greatly reduce the modeling time. Due to the advantages of *T-A* formulation, *T-A* formulation will be more and more widely used in various superconducting fields.

ACKNOWLEDGMENT

The authors would like to acknowledge the Robinson Research Institute (Victoria University of Wellington, Lower Hutt 5046, New Zealand) for providing the critical current data of SHS tape.

REFERENCES

[1] R. Schlosser, H. Schmidt, M. Leghissa, M. Meinert, "Development of high-temperature superconducting transformers for railway applications," *IEEE Trans. Appl. Supercond.*, vol. 13, no. 2, pp. 2325-2330, 2003.

[2] M. Iwakuma, K. Sakaki, A. Tomioka, T. Miyayama, M. Konno, H. Hayashi, H. Okamoto, Y. Gosho, T. Eguchi, S. Yoshida, Y. Suzuki, H. Hirai, Y. Iijima, T. Saitoh, T. Izumi, and Y. Shiohara, "Development of a 3 φ -66/6.9 kV-2 MVA REBCO superconducting transformer," *IEEE Trans. Appl. Supercond.*, vol. 25, no. 3, Art. no. 5500206, 2015.

[3] A. Ghabeli, M. Yazdani-Asrami, M. R. Besmi, S. Asghar Gholamian. Optimization of distributive ratios of apportioned winding configuration in HTS power transformers for hysteresis loss and leakage flux reduction[J]. *J. Supercond. Novel. Magn.*, vol. 28, no. 3, pp. 3463-3479, 2015.

[4] M. Yazdani-Asrami, M. Staines, G. Sidorov, M. Daviesa, J. Baileya, N. Allpressc, N. Glassonc, S. Asghar Gholamian. Fault current limiting HTS transformer with extended fault withstand time[J]. *Supercond. Sci. Technol.*, vol. 32, no. 3, Art. no. 035006, 2019.

[5] W. Song, Z. Jiang, M. Staines, R. A. Badcock, J. Zhang, "Design of a single-phase 6.5 MVA/25 kV Superconducting traction transformer for Chinese Fuxing high-speed train," *Int. J. Elect. Power Energy Syst.*, vol. 119, Art. no. 105956, 2020.

[6] D. Hu, M. D. Ainslie, J. Zhou, and D. A. Cardwell, "3D modelling of all-superconducting synchronous electric machine by the finite element method," in *Proc. COMSOL Conf.*, Cambridge, U. K., Sep, 2014, pp. 1-7.

[7] W. Song, Z. Jiang, X. Zhang, M. Staines, R.A. Badcock, J. Fang, Y. Sogabe, N. Amemiya, "AC loss simulation in a HTS single-phase 1 MVA transformer using H formulation," *Cryogenics*, vol. 94, pp. 14-21, 2018.

[8] W. Song, Z. Jiang, M. Staines, S. Wimbush, R. Badcock and J. Fang, "AC Loss Calculation on a 6.5 MVA/25 kV HTS Traction Transformer With Hybrid Winding Structure," *IEEE Trans. Appl. Supercond.*, vol. 30, no. 4, pp. 1-5, Art no. 5500405, 2020.

[9] V. M. R. Zermeno, F. Grilli, F. Sirois, "A full 3D time-dependent electromagnetic model for Roebel cables," *Supercond. Sci. Technol.*, vol. 26, Art. no. 052001, 2013.

[10] J. Geng, T. A. Coombs, "Modeling methodology for a HTS flux pump using 2D H-formulation," *Supercond. Sci. Technol.*, vol. 31, Art. no. 125015, 2018.

[11] Y. Jia, D. A. Mark, D. Hu. J. Yuan, "Numerical simulation and analysis of a saturated-core-type superconducting fault current limiter," *IEEE Trans. Appl. Supercond.*, vol. 27, no. 4, pp. 1-5, Art. no. 560805, 2017.

[12] Z. Wang, Y. Tang, L. Ren, J. Li, Y. Xu, Y. Liao, X. Deng, "AC loss analysis of a Hybrid HTS magnet for SMES Based on H-formulation," *IEEE Trans. Appl. Supercond.*, vol. 27, no. 4, pp. 1-5, Art. no. 4701005, 2017.

[13]H. Zhang, M. Zhang, W. Yuan, "An efficient 3D finite element model based on T-A formulation for superconducting coated conductors," *Supercond. Sci. Technol.*, vol. 30, Art. no. 024005, 2017.
[14]F. Liang, S. Venuturumilli, H. Zhang, M. Zhang, J. Kvitkovic, S. Pamidi, Y. Wang, W. Yuan, "A finite element model for simulating second generation high temperature superconducting coils/stacks with large number of turns," *J. Appl. Phys.*, vol. 122, no. 3, pp. 1-10, Art. no. 043903, 2017.
[15]F. Huber, W Song, M Zhang, G. Francesco. The T-A formulation: an efficient approach to model the macroscopic electromagnetic behaviour of HTS coated conductor applications[J]. *Supercond. Sci. Technol.*, vol. 35. No. 4, Art. no. 043003, 2022.
[16]C. R. Vargas-Llanos, S. Lengsfeld, F. Grilli, "T-A Formulation for the Design and AC Loss Calculation of a Superconducting Generator for a 10 MW Wind Turbine," *IEEE Access.*, vol. 8, pp. 208767-208778, 2020.
[17]Y. Yang, H. Yong, X. Zhang, Y. Zhou, "Numerical Simulation of Superconducting Generator Based on the T–A Formulation," *IEEE Trans. Appl. Supercond.*, vol. 30, no. 8, pp. 1-11, Art. no. 5207611, 2020.
[18]G. D. Santos, F. Sass, G. G. Sotelo, F. Fajoni, C. A. Baldan, E. Ruppert, "Multi-objective optimization for the superconducting bias coil of a saturated iron core fault current limiter using the T-A formulation," *Supercond. Sci. Technol.*, vol. 34, Art. no. 025012, 2021.
[19]Y. Wang, M. Zhang, F. Grilli, Z. Zhu, W. Yuan, "Study of the magnetization loss of CORC® cables using a 3D T-A formulation," *Supercond. Sci. Technol.*, vol. 32, Art. no. 025003, 2019.
[20]Z. Wen, H. Zhang, M. Mueller, "Sensitivity analysis and machine learning modelling for the output characteristics of rotary HTS flux pumps," *Supercond. Sci. Technol.*, vol. 34, Art. no. 125019, 2021.
[21]E. B. Juarez, V. M. R. Zermeño, F. Trillaud, F. Grilli, "Real-time simulation of large-scale HTS systems: Multi-scale and homogeneous models using the T–A formulation," *Supercond. Sci. Technol.*, vol. 32, Art. no. 065003, 2019.
[22]Y. B. Kim, C. F. Hempstead, A. R. Strnad, "Critical persistent currents in hard superconductors," *Phys. Rev. Lett.*, vol. 9, pp. 306-309, 1962.
[23]Z. Jiang et al., "AC Loss Measurements in a Hybrid REBCO/BSCCO Coil Assembly," *IEEE Trans. Appl. Supercond.*, vol. 27, no. 6, pp. 1-7, Art no. 5900707, 2017.